INL/JOU-17-42001-Revision-0

Detailed Measurements of Local Thickness Changes for U-7Mo Dispersion Fuel Plates with Al-3.5Si Matrix After Irradiation at Different Powers in the RERTR-9B Experiment

Dennis D. Keiser, Jr., Walter Williams, Adam Robinson, Dan Wachs, Curtis Clark, Doug Crawford

July 2017

The INL is a U.S. Department of Energy National Laboratory
operated by Battelle Energy Alliance

Idaho National Laboratory

INL/JOU-17-42001-Revision-0

Detailed Measurements of Local Thickness Changes for U-7Mo Dispersion Fuel Plates with Al-3.5Si Matrix After Irradiation at Different Powers in the RERTR-9B Experiment

Dennis D. Keiser, Jr., Walter Williams, Adam Robinson, Dan Wachs, Curtis Clark, Doug Crawford

July 2017

Idaho National Laboratory
Idaho Falls, Idaho 83415

http://www.inl.gov

Prepared for the
U.S. Department of Energy

Under DOE Idaho Operations Office
Contract DE-AC07-05ID14517

Detailed measurements of local thickness changes for U-7Mo dispersion fuel plates with Al-3.5Si matrix after irradiation at different powers in the RERTR-9B experiment

Dennis D. Keiser Jr. *, Walter Williams, Adam Robinson, Dan Wachs, Glenn Moore, Doug Crawford

Nuclear Fuels and Materials Division, Idaho National Laboratory, P. O. Box 1625, Idaho Falls, ID 83415-6146 USA

ABSTRACT

The Materials Management and Minimization program is developing fuel designs to replace highly enriched fuel with fuels of low enrichment. Swelling is an important irradiation behavior that needs to be well understood. Data from high resolution thickness measurements performed on U-7Mo dispersion fuel plates with Al-Si alloy matrices that were irradiated at high power is sparse. This paper reports the results of detailed thickness measurements performed on two dispersion fuel plates that were irradiated at relatively high power to high fission densities in the Advanced Test Reactor in the same RERTR-9B experiment. Both plates were irradiated to similar fission densities, but one was irradiated at a higher power than the other. The goal of this work is to identify any differences in the swelling behavior when fuel plates are irradiated at different powers to the same fission densities. Based on the results of detailed thickness measurments, more swelling occurs when a U-7Mo dispersion fuel with Al-3.5Si matrix is irradiated to a high fission density at high power compared to one irradiated at a lower power to high fission density.

1. Introduction

The Materials Management and Minimization (M3) program is collaborating with countries around the world to develop low-enriched uranium (LEU) U-Mo fuels for application in research and test reactors [1]. These fuels will be used to replace current fuels that use high-enriched uranium (HEU). One type of fuel being developed is a U-Mo dispersion fuel for application in European reactors, and the performance of this fuel during irradiation is of great interest. One area of research is to improve understanding of how the rate of thickness change for an as-fabricated U-Mo dispersion fuel plate during irradiation is affected by parameters other than just fission density. As fission density is increased during irradiation, the thickness of U-Mo dispersion fuel plates increase. A large contributor to this thickness change is the swelling of the U-Mo fuel particles, due to increasing amounts of solid and gaseous fission products in the fuel. Other contributing factors can be volume changes due to the U-Mo/matrix interaction layers that can form during irradiation and any volume changes due to porosity formation in the fuel meat (possibly due to fission gases leaving the U-bearing phases that enter the fuel meat and coalesce to form pores).

Typically the thickness change of a fuel plate is termed “fuel swelling” and a curve is drawn where the fuel swelling only depends on the fission density achieved by the fuel [2]. Yet based on the literature, other phenomena are known to impact the fission gas behavior in a nuclear fuel, which in turn can impact fuel swelling. As stated by Olander, fission gas behavior during irradiation of a nuclear fuel is affected by parameters like temperature, matrix stress, fission rate, irradiation time or burnup, fuel properties, vapor pressure, surface tension, surface and bulk diffusion, creep strength, fission gas properties, nuclear yields, dislocation density, grain size, restructuring, crack pattern, and fuel microstructure [3]. Therefore, it is of interest to gain understanding as to how some of these other parameters impact the swelling behavior of U-Mo dispersion fuels.

☆ This manuscript has not been published elsewhere and has not been submitted simultaneously for publication elsewhere.

* Corresponding author.
E-mail address: dennis.keiser@inl.gov (D.D. Keiser).

The goal of this particular research is to investigate the effect of power on the swelling behavior of irradiated U-Mo/Al-Si dispersion fuels. Fuels that are irradiated at higher power can be exposed to higher temperature, higher fission rate, different matrix stress, different vapor pressure and surface tension, higher diffusion rates, different creep strength, different fission gas properties, etc. For this investigation, detailed thickness measurements were performed on fuel plates R6R018 and R6R038 that were irradiated in the RERTR-9B experiment in the Advanced Test Reactor (ATR), located in Idaho Falls, Idaho. Due to its location in the core, R6R018 was irradiated at a higher power than was R6R038, and both plates were irradiated to relatively high fission densities. Each fuel plate consisted of U-7Mo fuel particles dispersed in an Al-3.5Si matrix, and they were manufactured the same way. The thickness measurements were performed using the same remote fuel metrology system. This paper discusses the results of the non-destructive examinations performed on fuel plate sections from these fuel plates that were irradiated to high fission density at two different powers, including visual inspection and detailed thickness measurments. The results of performed destructive examinations will be described in a follow-on paper. Comments will be made as to how an increase in reactor power appears to increase the fuel swelling observed for U-Mo/Al-3.5Si fuel plates irradiated in ATR.

2. Experimental

2.1. Fabrication

Fabrication of RERTR-9B fuel plates is discussed in Ref. [4]. The fuel was produced using a blend of highly-enriched uranium (HEU), depleted uranium (DU), and molybdenum (Table 1). The materials were blended using an arc-melting furnace with multiple melts and ingot flips to ensure homogenization of the alloy blend. A total of three buttons were produced of the same (nominally) alloy and uranium enrichment. Each of the three buttons was cast into pins for atomization.

Atomization of the powder was conducted using a standard rotating electrode process atomizer in an inert atmosphere glovebox. The oversize material (>106 μm) was recycled along with stub portions of the cast pins by remelting into buttons and casting into pins. Chemical analysis was performed on several grab samples of the final powder and the results can be seen in Table 2.

Aluminum matrix material used in the R6R018 and R6R038 dispersion plates consisted of an alloyed binary material gas atomized to produce a powder. This powder had a nominal composition of 3.5% Si. This material was vacuum degassed prior to compaction according to a standard procedure. Final chemical analysis for this material is shown in Table 3.

The powder size distribution employed for producing the fuel plates is presented in Table 4.

Fuel meat compacts were fabricated in an inert atmosphere glovebox. The fuel and matrix powders were blended in a glass vial by hand shaking for two minutes. The blended powder was poured into a die measuring 17.75 mm by 22.25 mm. Prior to loading the powder, the die was lubricated with a thin coat of aerosol zinc stearate. The die was compacted in a hydraulic press to 213.5 kN and the pellet was removed from the die, crushed with a mortar and pestle, and then recompacted as before to render the final pellet. Thickness of this pellet was measured as 0.2 cm. The compact masses are shown in Table 5.

The cladding plate hardware consisted of two Al-6061 sheet stock. A thin cover plate and a thicker plate with a machined recess sized to fit the fuel compact. The sheets were sized so that the assembled pellet was midway between the two faces of the rolling assembly. The cladding was cleaned using a wire brush to remove any gross scale from the plates followed by a degreasing (acetone and ethanol), sodium hydroxide and nitric acid, and assorted rinses. The fuel compacts were loaded into the aluminum hardware within 1 day of cleaning. The assembly was then welded closed for rolling.

The plates were rolled using a large two-high rolling mill in conjunction with a plate-heating furnace. Rolling takes place within 1 day of the assembly/welding. The rolling schedule/heating times are identified in Table 6. This rolling schedule has been shown to deliver plates at the desired thickness (1.375 mm ± 50 μm). The final plates received a 4:1 reduction, had a uranium density of around 8.5 gU/cm^3, and 15% of the powder was >90 μm.

After final rolling the furnace was cooled to 485 °C, the plate was placed inside the furnace, and heated for 30 min. After the heating step the plate was removed from the furnace, cooled in air, and examined for blisters. The plates passed the blister inspection.

The rolled plate then underwent radiography to determine the location of the fuel zone within the plate and to determine if there

Table 1
Materials used in fuel production.

Material	Purity (%)	Enrichment (%U^{235})
HEU	99.74	93.17
DU	99.8	0.20
Molybdenum	99.95	N/A

Table 2
Results of chemical analysis of final fuel powder.

Item	Amount (wt.%)
Molybdenum	6.99
Total Uranium	93.01
U^{235} (of Total U)	58.14

Table 3
Results of chemical analysis of matrix powder.

Element	Amount	Element	Amount	Element	Amount
Si	3.41	Fe	0.08	Cu	<0.01
Mn	<0.01	Mg	0.001	Cr	<0.01
Ni	<0.01	Zn	<0.01	Ti	<0.01
Sn	<0.01	Pb	<0.01	Al	Remainder

Table 4
U-7Mo powder size distribution.

Powder Size (μm)	Wt.%
90–106	15
75–90	43
63–75	13.2
53–63	5.3
45–53	3.1
<45	20.4

Table 5
Compact materials and corresponding weights.

Material	Powder Mass (g)	
	Starting	Final (Calculated)
Matrix (Al-3.5Si)	0.921	0.916
Small Fuel Alloy (<90 μm)	5.540	5.510
Large Fuel Alloy (90–106 μm)	0.978	0.973

Table 6
Rolling and heating schedule.

Pass No.	Thickness (in.) Target	Reduction	Heating Soak		
			Time	Total	Temp
0	0.222	0%	20	20	500
1	0.189	15%	10	30	500
2	0.160	15%	10	40	500
3	0.128	20%	10	50	500
4	0.103	20%	10	60	500
5	0.082	20%	5	65	500
6	0.066	20%	5	70	500
7	0.066	0%	5	75	500

is excessive fuel out of zone. Using the radiography and an overlay template the plates were marked and sheared to their final size. After shearing to their final size the plates were sent again to radiography to determine fuel location, fuel out of zone, and fuel density. Both plates passed the radiography inspection.

2.2. Irradiation testing

The primary purpose of the RERTR-9B experiment was to enhance the understanding of how fuel behavior is affected by fission rate, temperature, fission density, slight composition shifts, and fuel density loading. The experiment consisted of four capsules (A–D), each containing eight plates. The plates are arranged in two rows of four in each capsule. Each plate is nominally 2.54 cm in width, 10.2 cm in height, and approximately 1.4 mm in thickness (with a target of 1.375 mm ± 50 μm). While the goal of the M3 program is to develop LEU fuels, the size of the mini-plates requires the use of HEU fuel in order to test prototypic conditions including power density and temperature. The RERTR-9 experiment was irradiated in the Advanced Test Reactor (ATR) with the capsule oriented such that one edge of the plates was facing the core center. Plates R6R018 and R6R038 were irradiated during cycles 140A, 140B, and 141A. The experiment was irradiated for 115 effective full power days (EFPD). These experiments were irradiated in the large-B position B-11. The orientation combined with the higher enrichment leads to self-shielding and a subsequent large fission density gradient across the 2.54-cm width of the plate. Plates R6R018 and R6R038 were located in the B-7 and D-7 position, respectively, of the RERTR-9B experiment.

Three computer codes (Monte Carlo N-Particle [MCNP], MCWO, and ORIGEN2) were used to calculate the as-run fuel fission neutron heat rates, power density, and U-235 burn-up. The three codes work together in the following methodology: MCNP calculates the nuclear reaction rates for U-235 (and other isotopes), MCWO then takes these rates and passes the information into an ORIGEN2 readable file, and ORIGEN2 then solves the system of equations that govern burnup to calculate the U-235 burn up for a given time step. After ORIGEN2 has finished the burn up calculation for the given time step the output (mass values of the isotopes from burn up) from ORIGEN2 is passed back through MCWO to create new atom densities and then the computational sequence is performed again until the end of the irradiation time frame. The plate average power and burn-up were calculated for five time intervals per cycle. The fission power density, heat flux, and burn-up were calculated for the fuel plates [5]. In Table 7 are presented the calculation values for fuel plate R6R018, since it was the highest burnup RERTR-9B fuel plate. Similar data was produced for the lower burnup R6R038 fuel plate, and more information on the irradiation parameters for the R6R018 and R6R038 fuel plates can be found in Ref. [5]. In Table 8, are listed the overall calculated irradiation conditions for the R6R018 and R6R038 fuel plates.

2.3. Thickness measurements

Profilometry was performed using a remote fuel metrology system (see Fig. 1). This device used two opposing vertical Sony linear variable differential transformer (LVDT) probes that range over the area of a plate and obtain thickness measurements at any location (see Fig. 2). This was accomplished by selecting an automated measurement program to position the probes to collect the data in an incremented grid across the plate. The automated program used a pre-described plate size with an incremented number of samples in both the x and y direction to build the measurement grid. Two calibrated thickness standards of thicknesses 0.11 cm and 0.15 cm are mounted in a blank aluminum plate and stored with the plate checker. Before and after checking each plate, it was verified that the system is still within calibration to within 0.01 mm on both standards. A zero check was also performed and was within ±0.01 mm.

Due to the required use of an adaptor to hold mini-plates, some measurements near the edges of the plates are removed due to the probes contacting the rail of holder. This contact generates clearly invalid data exceeding 300% plate thickness change and is not included in any of the calculations or analysis. Graphical displays of the thickness measurements included throughout this report are not corrected for oxide buildup, which is predominantly fewer than 15 μm in thickness. These displays portray thickness change as only occurring in a singular direction, resulting in an increase in thickness. Due to the inability to distinguish thickness change of the front face from the rear face the graphs do not represent the physical appearance of the plate surface, but rather a total behavior at that location.

The term “fuel swelling” in this report is employed to reflect the phenomena that occur during irradiation that impact at some level the fuel meat thickness change including: swelling of the U-7Mo fuel (due to growth of solid and gaseous fission products), interaction layer swelling, growth of the lower-density interaction layer in thickness, the development of relatively large pores at the fuel/matrix and matrix/Al interfaces, creep, and sintering of the fuel particles. Fuel meat thickness change (swelling) in this study is represented as percent “fuel swelling” at a certain fission density, and it is determined using Equation (1). The fuel swelling (*Sf*) consists of the following: 1) t_p, the measured post irradiation thickness at a specific location. 2) t_{ox}, the thickness of the oxide layer at this location, disregarded in this study due to negligible thickness (less than ten microns). 3) t_{p0}, the pre-irradiation plate thickness from as-built reports. 4) t_{fe}, the equivalent fuel meat thickness. Where these values are not available, they are calculated from as built dimensions, density, and weight. The fuel volume fraction, calculated from areal density of pre-irradiation radiography, is used to calculate the equivalent fuel swelling.

$$S_f = \frac{\left(t_p - \frac{5}{12}t_{ox}\right) - t_{p0}}{\left(t_{fe}\right)V_f} \quad (1)$$

The high-resolution post irradiation thickness data in this study was collected on a grid with ~0.98 mm spacing over remaining plate. Each set of data handled individually to remove cladding-cladding regions as well as defects caused by prior destructive examination performed on sections taken from the center of the fuel plates.

Plate average fission density was generated with MCNP and scaled over the plate, using MCNP-calculated local-to-average ratios (L2ARs) where available. For dispersion type plates, these values are corrected using the volume fractions. The thickness data

Table 7
Power density, heat flux, and U-235 burn-up per interval for plate R6R018.

Cycle/Interval	Fission Power Density (W/cc)	Heat Flux (W/cm^2)	Cumulative U-235 Burn-up U-235/U-235$_{initial}$ (%)
Cycle 140A/02	11414.60	289.93	5.88%
Cycle 140A/03	10250.11	260.35	11.25%
Cycle 140A/04	10949.42	278.12	14.32%
Cycle 140B/02	9559.97	242.82	17.65%
Cycle 140B/03	10790.47	274.08	21.34%
Cycle 140B/04	10686.13	271.43	25.14%
Cycle 141A/02	9711.84	246.68	29.40%
Cycle 141A/03	9373.52	238.08	32.12%
Cycle 141A/04	10232.18	259.90	34.02%

Table 8
Calculated irradiation conditions for the R6R018 and R6R038 fuel plates.

Fuel Plate	Ave. Heat Flux (W/cm^2)	Peak Heat Flux (W/cm^2)	Peak Power Density (W/cc)	Ave. Fission Density (f/cm^3)	Peak Fission Density (f/cm^3)	Max Surface Temp (°C)	Ave. Surface Temp (°C)
R6R018	259.9	717.4	2.82×10^4	5.97×10^{21}	1.65×10^{22}	103.7	82.4
R6R038	213.9	581.8	2.29×10^4	4.67×10^{21}	1.27×10^{22}	106.7	89.3

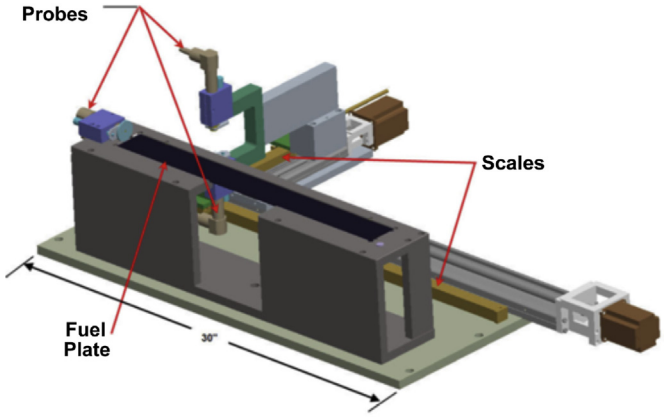

Fig. 1. Remote fuel metrology system.

has the most accurate recording for location; thus MCNP and gamma scan values for L2AR fission density are interpolated to fit thickness data.

3. Results

3.1. R6R018

Visual examination of the R6R018 plate after removal from the irradiation capsule showed no signs of excessive swelling or oxidation, blistering, or gross deformation. Fig. 3 shows the photographs taken of both the front and back of the plate during the examination. The lighter colored region of the plate over the fuel indicates a boehmite oxide layer indicative of a higher temperature during irradiation. Eddy current testing was performed to investigate the oxide thickness formation on the plate. The peak oxide observed was 21 μm with the average thickness being 3.6 μm.

Gamma scanning of the plate was conducted to verify gradient calculations and burn-up information. Gamma scans are performed in both the axial and transverse direction across the fuel plate. Plots of the gamma scan profiles collected can be seen in Fig. 4. The high power to low power edge ratio for the transverse gamma scan is approximately 2.4 while the top to bottom ratio for the axial scan is approximately 1.08. This agrees with the gradient calculations that showed ratios of approximately 2.5 and 1.1 for the transverse and axial gradients, respectively.

Initially, a small section was taken from the center of fuel plate R6R018 and used for destructive examination. The remaining two pieces were used for thickness measurements, and a photograph of the two R6R018 fuel plate sections employed for the thickness measurements are presented in Fig. 5.

Contour plots were generated from the thickness measurement data using MatLab to depict both fuel plate sections in terms of fission density at a specific location on the fuel plate and the fuel plate thickness measured as a function of fuel plate location. While the relative location of each thickness measurement is well documented, the absolute location (from plate edges) does not account for fuel location within the cladding. As such, these plots were used to align and crop the fuel region from the swelling measurements to the neutronics profile. In Fig. 6, the final contour plots are shown for the top fuel plate section, and in Fig. 7 the final contour plots are shown for the bottom fuel plate section. The maximum thickness was observed at a location about 4 mm from the bottom the fuel plate, (see Fig. 7 (b), near the peak fission density location).

The entirety of the collected data is used for swelling calculations because mini-plates do not have any subsections that are truly unconstrained, and in edge induced fuel creep, swelling is conserved as shown in the gamma scans where each peak is accompanied by a constrained low swelling region. A plot of these results for the top and bottom sections of the fuel plate are shown in Fig. 8(a). The plots produced for each half of the R6R018 plate overlap with each other and are in good agreement. In order to account for the uncertainties in local variations in fuel swelling due to geometric effects (fuel edges, fuel creep, etc.), preirradiation foil thickness variations, and uncertainties in the local calculated fission density values, the calculated fuel swelling values can be fit using a standard least squares analysis (see Fig. 8(b)). This is a more informative way of comparing different plates as it lessens the location dependency. By grouping the data by fission density or fitting the behavior by standard least squares, we are able to better estimate the fuel swelling, regardless of its location in a fuel plate. This statistical analysis includes a 95% confidence interval for the locally collected data. This method was also applied to the fit itself and is presented in Fig. 8(c).

For comparison, other data available in the literature for other irradiated U-7Mo dispersion fuel plates with similar characteristics have been included on the plots in Fig. 8. This literature data was produced with a similar device called the BONAPARTE bench. U-

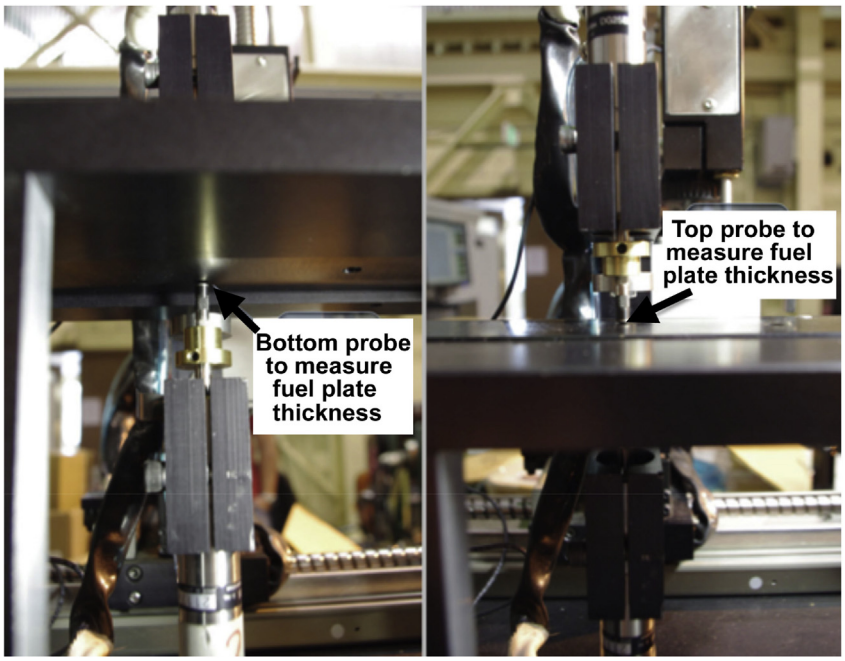

Fig. 2. LVDT probes during measurement.

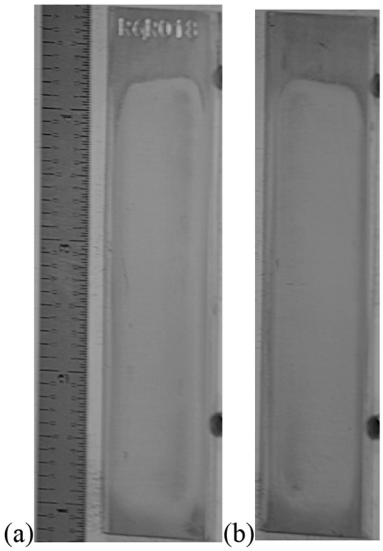

Fig. 3. Visual examination photographs of the (a) front and (b) back of plate R6R018.

7Mo/Al-4Si dispersion fuel plates were irradiated in the EFUTURE experiment in the BR-2 reactor and then run through the BONAPARTE measurement bench to get thickness data [6], and a fuel plate with Si-coated U-7Mo fuel particles (600 nm-thick Si coating) in an Al matrix that had similar characteristics compared to the R6R018 fuel plate was irradiated in the SELENIUM experiment in the BR-2 reactor and then analyzed using the same BONAPARTE bench [7]. The EFUTURE fuel plates formed blisters at local regions of the fuel plates that had been exposed to fission densities near 5.0×10^{21} fissions/cm^3, but the fuel plates irradiated in SELENIUM did not. Besides the data for the individual fuel plates E-FUTURE U7MC4111 and SELENIUM U7MD1221, data is available for two U-7Mo dispersion fuel plates irradiated in the AFIP-1 experiment in ATR [8]. One fuel plate had an Al-2Si alloy fuel meat and the other had an AA4043 alloy (~4.8 Si) fuel meat. Detailed thickness measurements were performed using a UT scanner in the ATR canal. Fuel plate 1B5, which had the AA4043 fuel meat matrix with the highest Si concentration, is also plotted in Fig. 8 for comparison. It can be seen in the plot of the "binned" R6R018 data shown in Fig. 8(a) that the two fuel plate sections exhibited more fuel swelling in general compared to EFUTURE, SELENIUM, and AFIP-1 fuel plates at similar fission densities. Also, the deviation from linearity of the fuel swelling versus fission density plot that was observed for the EFUTURE and SELENIUM fuel plates at a fission density near 4.5×10^{21}fissions/cm^3 was not observed for R6R018 (or AFIP-1 fuel plate 1B5). The results for another fuel plate (SELENIUM 1a) irradiated at a relative low power have recently been reported [9], but were not plotted since it had a similar profile as SELENIUM and no change in slope at 4.5×10^{21}fissions/cm^3.

3.2. R6R038

Like was the case for fuel plate R6R018, a section was removed from the middle of the R6R038 fuel plate for destructive examination. A photograph of the remaining R6R038 fuel plate sections employed for the thickness measurements is presented in Fig. 9.

In the contour plots that were generated using MatLab for the top and bottom R6R038 fuel plate sections (see Figs. 10 and 11), it can be seen that, as was the case for R6R018, the maximum thicknesses were measured at the highest fission density locations (near corners and edges of the high-flux side of the fuel plate).

Plots of the thickness measurement results for the top and bottom sections of R6R038 are shown in Fig. 12. Like was plotted for fuel plate R6R018, the data points for the individual measurements (a), the 95% confidence bands for the data (b) and the curve fit (c) are plotted. Overall, the R6R038 fuel swelling change measured for different values of fission density are significantly less than those for R6R018. However, the data from the two R6R038 fuel plate sections at lower fission densities are similar to the EFUTURE and SELENIUM fuel plates, except that no discontinuity in the plot of thickness change for the R6R038 fuel plate occurred at just over 4.5×10^{21} fissions/cm^3, like was the case for the EFUTURE,

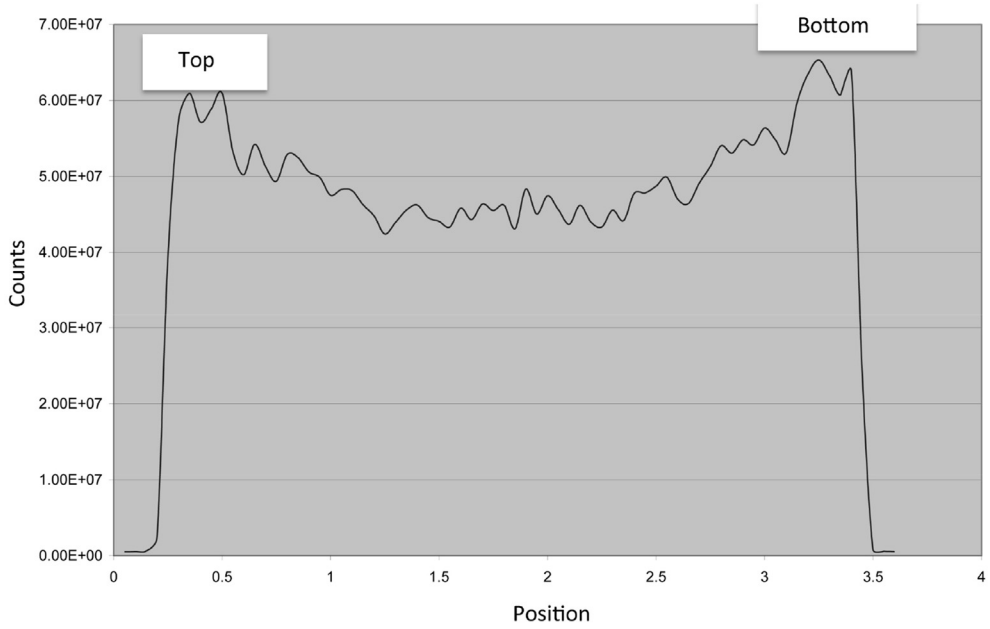

(a)

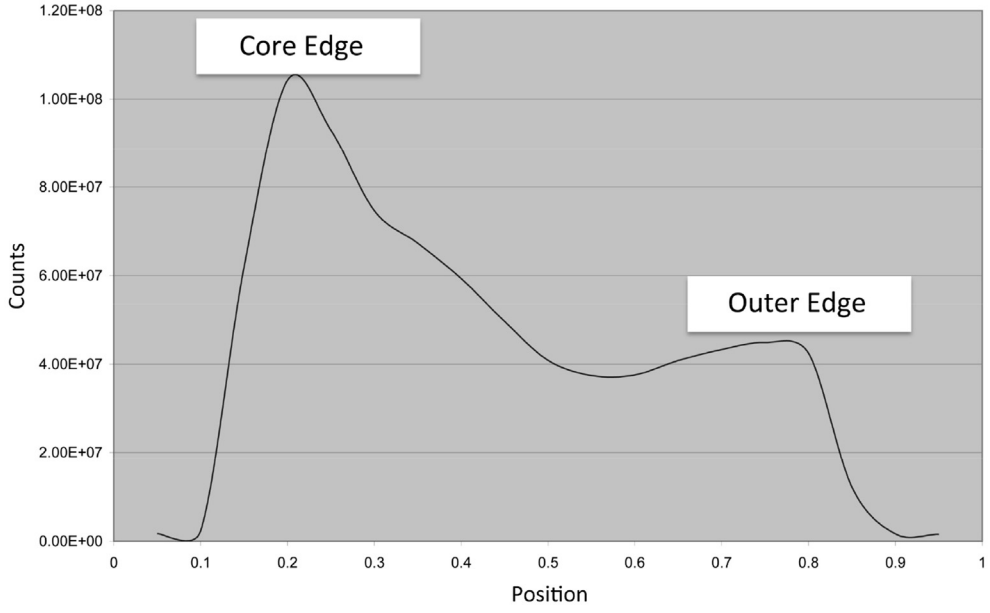

(b)

Fig. 4. Fuel plate R6R018 gamma scan results along the length of the plate (a) and along the width (b).

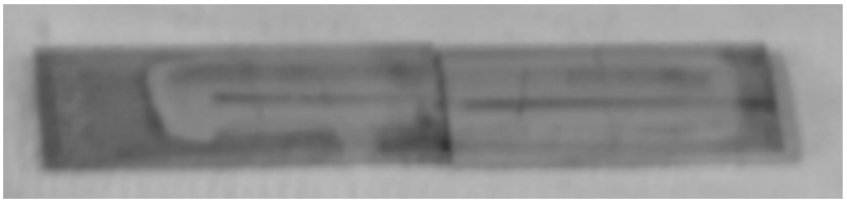

Fig. 5. R6R018 after section at mid-plane was removed for optical metallography. (The image quality is low due to the impact of taking an image in a hot cell).

SELENIUM, fuel plates. Unlike R6R018, the fit for each section of R6R038 do not overlap with one another, however they remain in relatively good agreement.

Fig. 13 shows the plots for the top and bottom sections for fuel

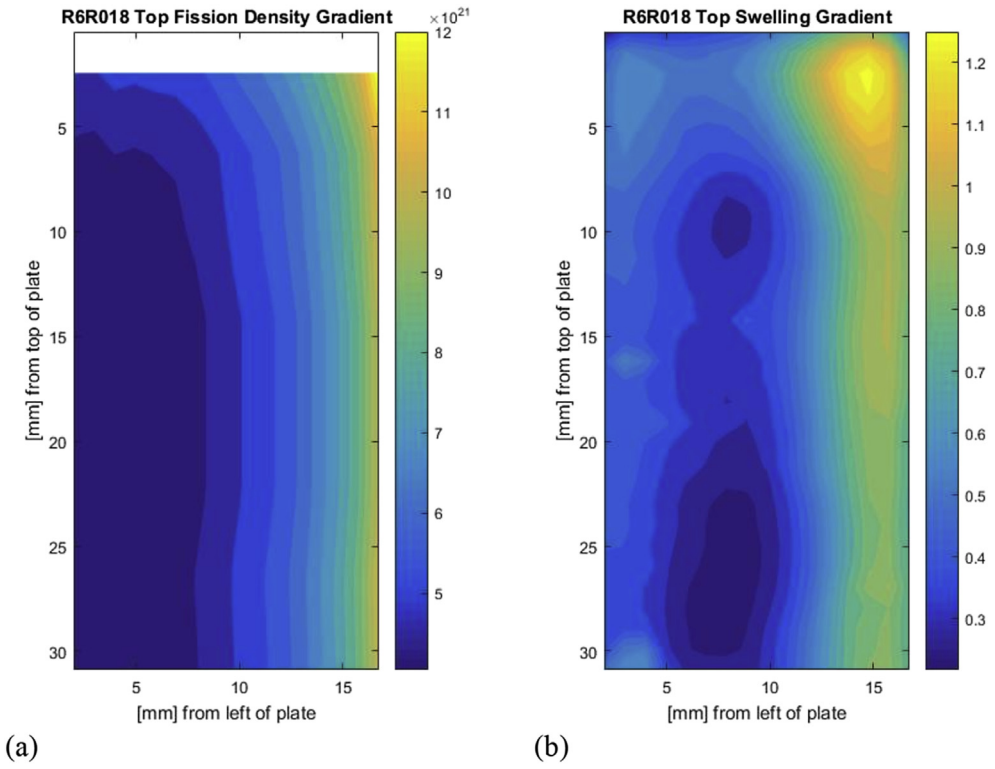

Fig. 6. Color contoured images showing (a) the variation of fuel phase fission density and (b) the variation of fuel swelling as a function of location on the top of fuel plate R6R018.

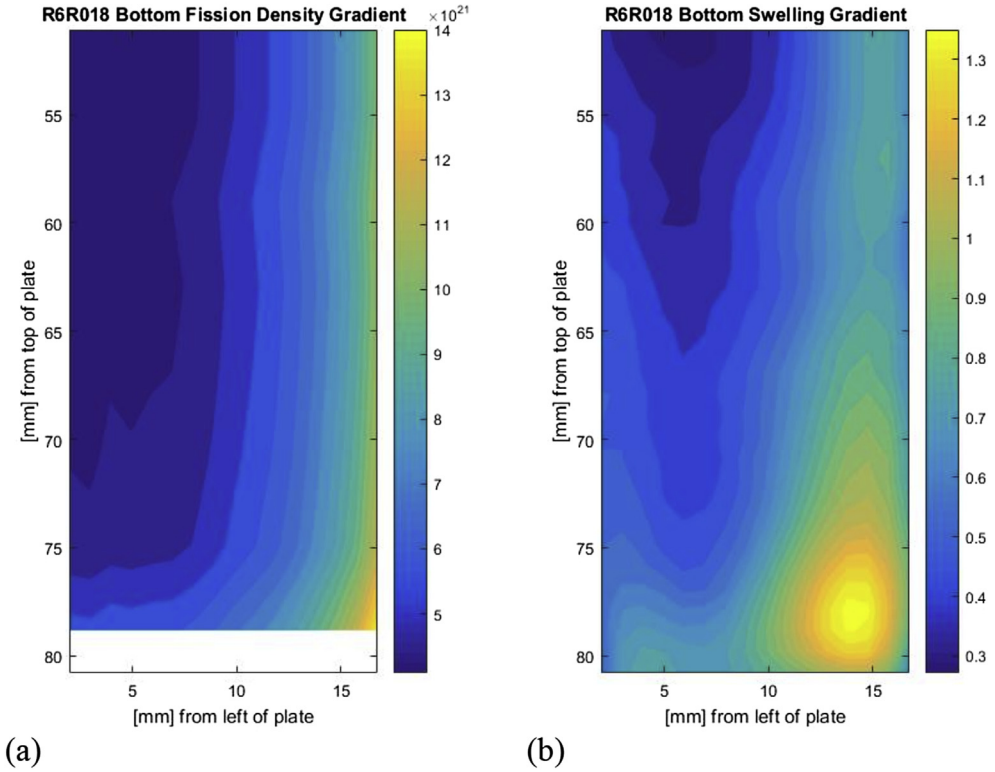

Fig. 7. Color contoured images showing (a) the variation of fuel phase fission density and (b)the variation of fuel swelling as a function of location on the bottom of fuel plate R6R018.

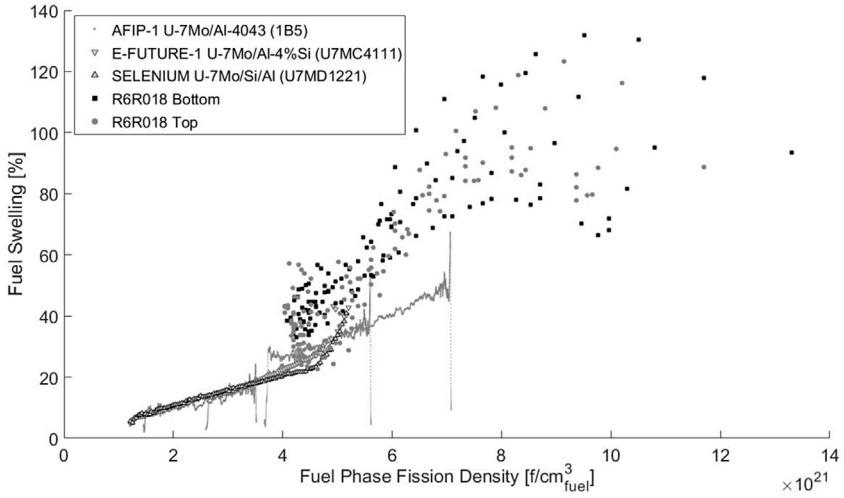

(a)

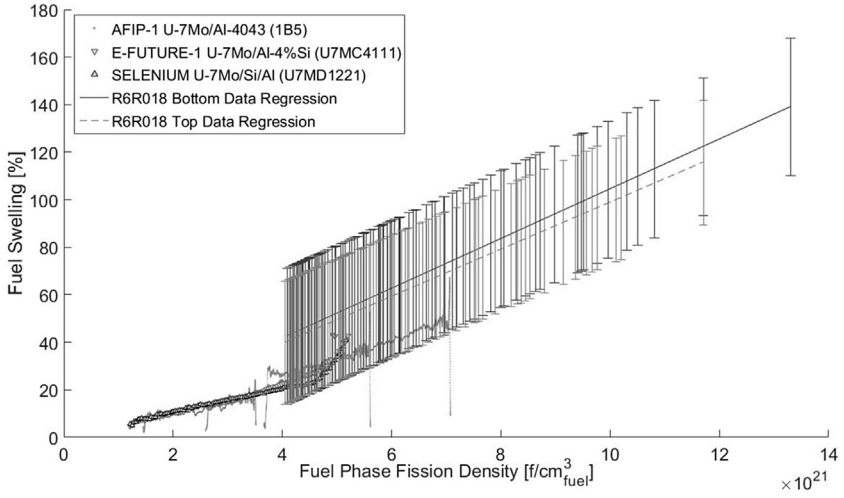

(b)

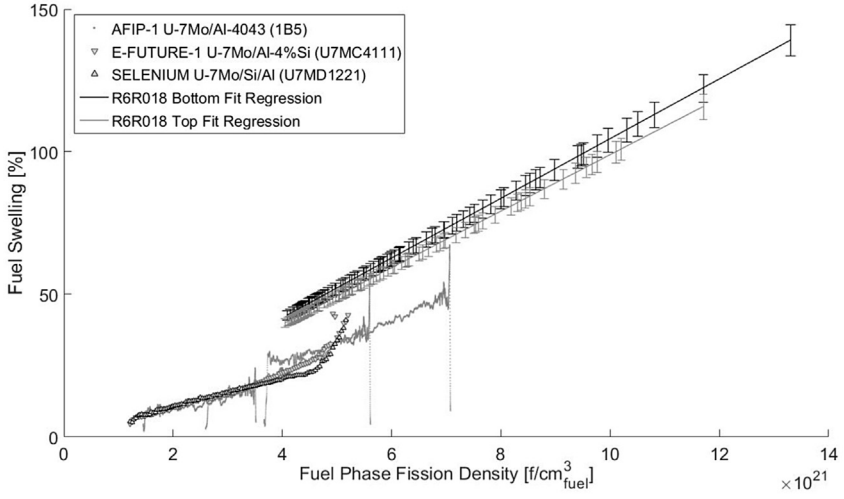

(c)

Fig. 8. (A) Plot of percent fuel swelling as a function of fuel phase fission density for fuel plate R6R018. (B) Linear Regression Plot of percent fuel swelling change as a function of fuel phase fission density for R6R018 including a 95% confidence band of the data. (C) Linear Regression Plot of percent fuel swelling change as a function of fuel phase fission density for R6R018 including a 95% confidence band of the fit. Data curves for fuel plates AFIP-1 1B5, E-FUTURE U7MC4111 and SELENIUM U7MD1221 are included for comparison on all plots.

Fig. 9. Photograph of the R6R038 fuel plate sections used for thickness measurements.

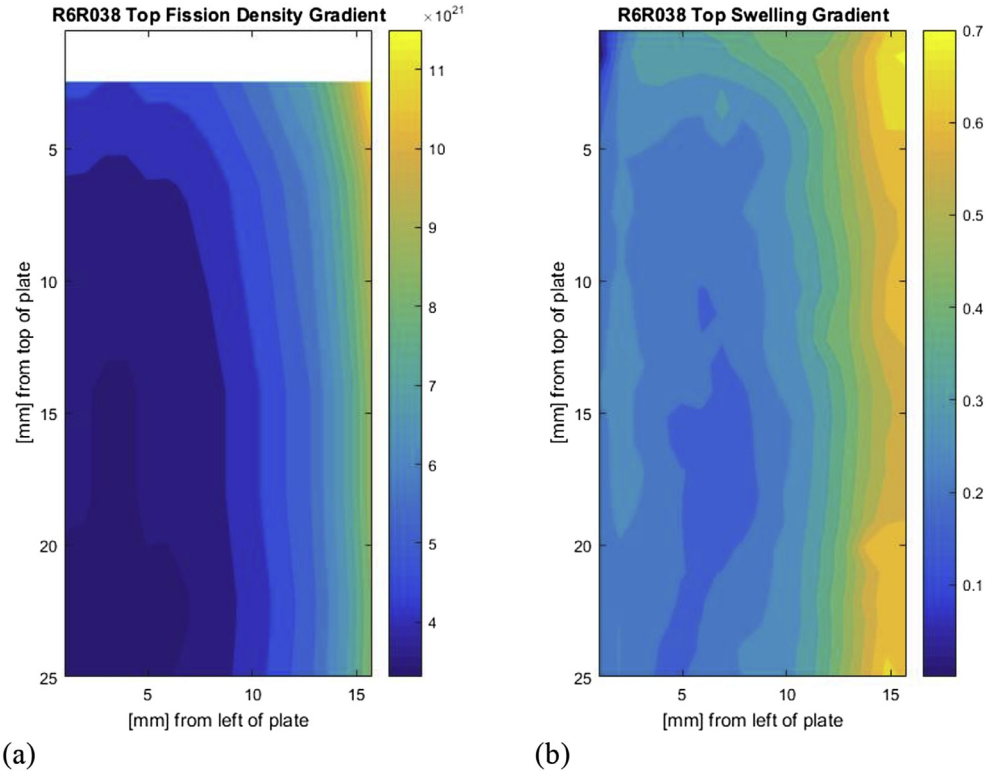

Fig. 10. Color contoured images showing (a) the variation of fuel phase fission density and (b) the variation of fuel swelling as a function of location on the top of fuel plate R6R038.

plate R6R018 and R6R038 all presented on one graph, along with those reported for E-FUTURE U7MC4111, SELENIUM U7MD1221, and AFIP-1 1B5 fuel plates. SELENIUM 1a results are not plotted since they are similar to the SELENIUM fuel plate except with no change in slope. This plot highlights the fact that as fission density is increased the difference in the measures swelling values for the R6R018 fuel plates sections and the R6R038 fuel plate sections increases. By extrapolating swelling values to the lowest values of fission density (around 2.5×10^{21} fissions/cm^3), there appears to not be much difference in the swelling values for the different R6R018 and R6R038 fuel plate sections. However, at higher fission density more swelling occurs for R6R018 vis-a-vis R6R038. At a fission density of around 4.2×10^{21} fissions/cm^3, the swelling that was measured could be as low as around 18% (R6R038) or as high as around 40% (R6R018). At a fission density of 6.0×10^{21} fissions/cm^3, the swelling value could be just over 20% (R6R038) or just over 60% (R6R018). At the highest fission density values (over 10.0×10^{21} fissions/cm^3) the difference becomes quite significant (close to double the swelling for R6R018 compared to R6R038).

In order to correlate observed swelling behavior at a specific location on a fuel plate with different irradiation parameters, calculations were performed for fuel plates R6R018 and R6R038 using the PLATE code. This computer code has been described by Hayes et al. [10] Particularly, fission density, fission rate, power, and temperature were of interest. In particular, the location of maximum fuel plate thickness measured for either fuel plate was identified, which was observed to be at about 6 mm from the bottom of fuel plate R6R018. Calculations were then made along a transverse line at that specific location for each fuel plate so that comparisons could be made. At the 6 mm location for fuel plate R6R018, the highest observed fuel particle fission density, maximum fission rate, maximum heat flux, and end-of-life temperature are 1.4×10^{22} fissions/cm^3, 9.6×10^{14} fissions/cm^3 sec, 458 W/cm^2, and 282 °C, respectively. At the 6 mm location for fuel plate R6R038, the highest observed fuel particle fission density, maximum fission rate, maximum heat flux, and end-of-life temperature are 1.1×10^{22} fissions/cm^3, 8.4×10^{14} fissions/cm^3 sec, 320 W/cm^2, and 178 °C, respectively. R6R018 was exposed to the most aggressive irradiation conditions, and fuel plate R6R038 had no locations where such aggressive conditions were reached.

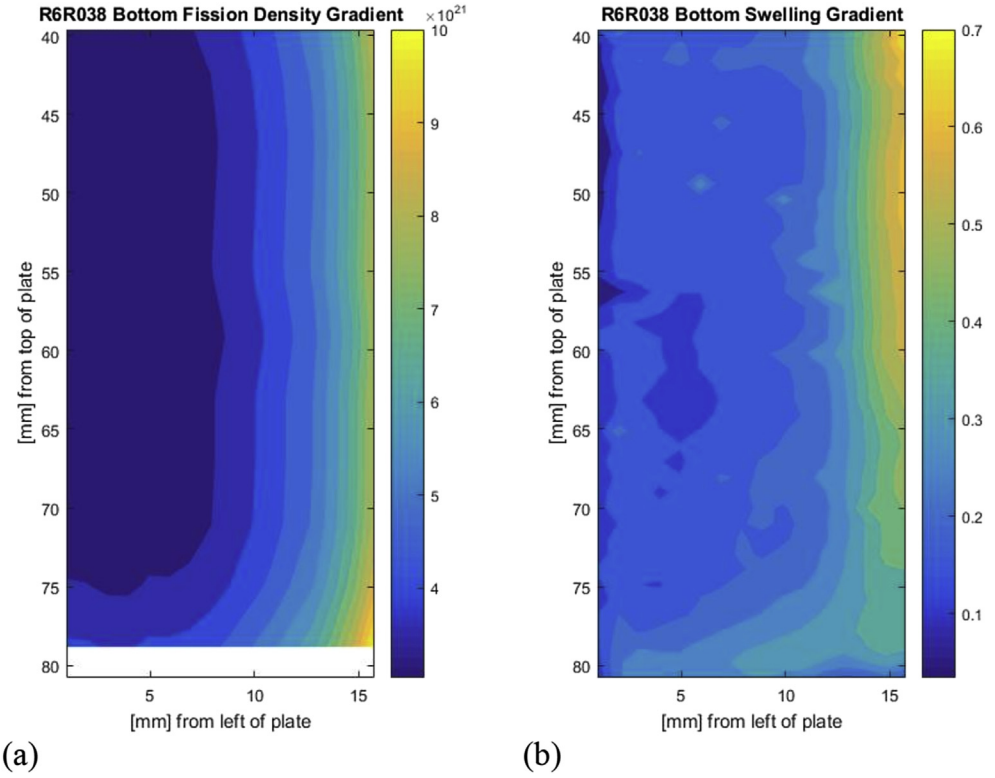

Fig. 11. Color contoured images showing (a) the variation of fuel phase fission density and (b) the variation of fuel swelling as a function of location on the bottom of fuel plate R6R038.

Overall, the swelling was higher for fuel plate R6R018 at all fission densities, and this can be seen in the fuel swelling plots. Calculations showed that parameters like fission rate (power) and temperatures at a certain fission density were higher for R6R018, and they appear to impact the final observed fuel swelling.

When comparing calculated parameter results of R6R018 and R6R038, where the peak values occurred at the edges of the fuel plates, with those reported for EFUTURE, SELENIUM, SELENIUM 1a, and AFIP-1 (see Table 9), which had less edge effects, it can be seen that even though R6R018 and R6R038 were irradiated at conditions more aggressive than the EFUTURE and SELENIUM fuel plates, they did not exhibit signs of breakaway swelling. The R6R038 fuel plate achieved higher peak heat flux and peak fission density than did the EFUTURE and SELENIUM fuel plates, and it exhibited similar swelling behavior, whereas, the R6R018 fuel plate in addition had a higher fission rate, and it exhibited much higher swelling. Even though the AFIP-1 1B5 and SELENIUM 1a fuel plates had relatively low heat fluxes of 250 W/cm^2 and 350 W/cm^2, respectively, they exhibited swelling that was similar to fuel plate R6R038. Therefore, it appears that below a certain threshold of power (and possibly other parameters), the swelling behavior of dispersion fuel comprised of U-7Mo fuel particles dispersed in Al-Si matrices with around 4 wt% Si may be fairly consistent.

4. Discussion

Many phenomena are transpiring during the irradiation of the R6R018 and R6R038 fuel plates that can affect the changing thickness of the fuel plates. Some of these include swelling of the U-7Mo fuel (due to growth of solid and gaseous fission products) [11]; interaction layer swelling; growth of the interaction layer in thickness; the development of relatively large pores at the fuel particle/matrix, fuel particle/interaction layer, interaction layer/matrix, and fuel particle/fuel particle interfaces; creep; and sintering of the fuel particles. Some phenomena inherent to testing in ATR that can affect thickness change of a fuel plate include: constraint from the rails in which the fuel plates were swaged, the growth of AA6061 cladding corrosion product (that can affect fuel temperature), and coolant pressure.

Due to the fact that many variables can change between fuel plates, it is very difficult to understand the impact of individual variables by themselves. The benefit of comparing the fuel swelling behavior between R6R018 and R6R038 is that they were fabricated in the same way (resulting in analogous starting microstructures); they were in the same experiment, with the same orientation to the core, and saw similar constraint from the rails, oxide growth on the cladding, and coolant pressure effects; and the thickness measurements were made using the same measurement device and methodologies so the variable of taking measurements using different equipment and approaches was removed. The main differences between the plates were in the irradiation conditions. Due to its location in the core, R6R018 had specific locations where it was irradiated at more aggressive conditions compared to R6R038. As discussed earlier, R6R018 achieved higher fission densities, fission rates, power, and temperature. The result of these differences was a higher rate of local fuel swelling during irradiation.

Starting at the lowest stages of irradiation, R6R018 exhibited more fuel swelling than the R6R038 fuel plate, and the final observed swelling difference was higher at higer fission density. As a result, the slope of the line for thickness change as a function of fuel meat fission density was higher for R6R018 vis-a-vis R6R038. Since R6R018 was exposed to a higher fission rate, more defects (dislocations, vacancies, Frenkel defects, etc.) were likely produced in the U-7Mo fuel and the U-bearing interaction layer and at a faster rate, which can accelerate the effects of specific phenomenon (e.g., diffusion and creep).

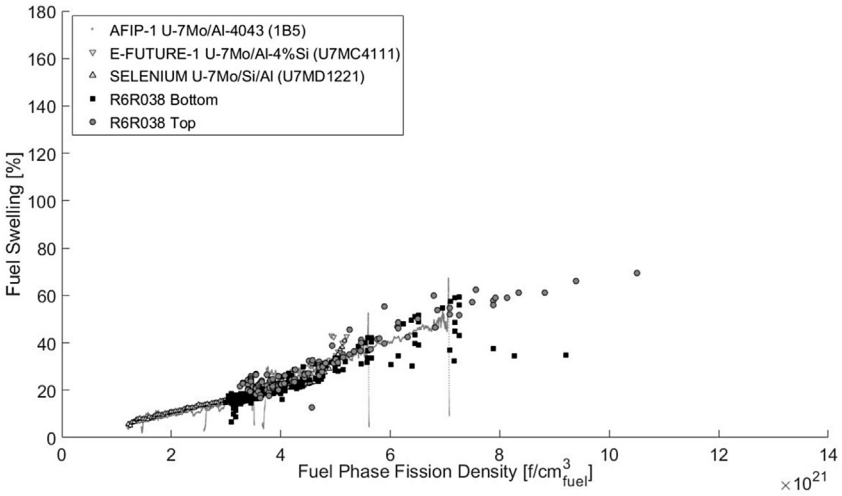

(a)

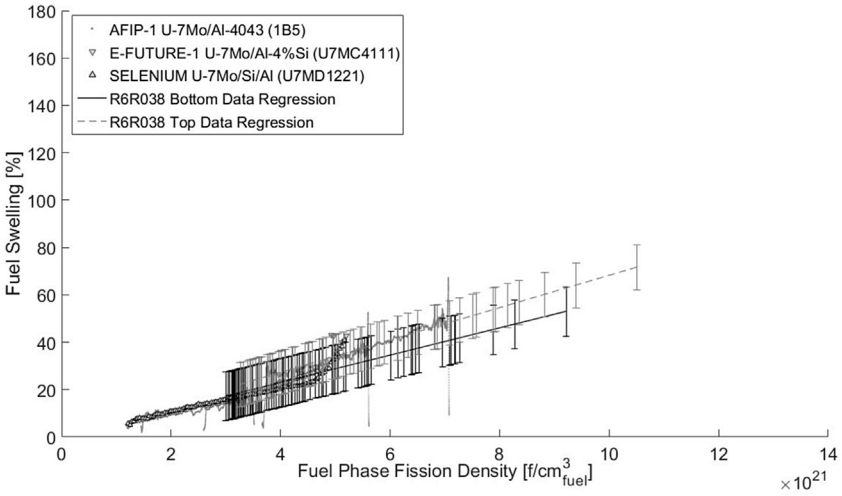

(b)

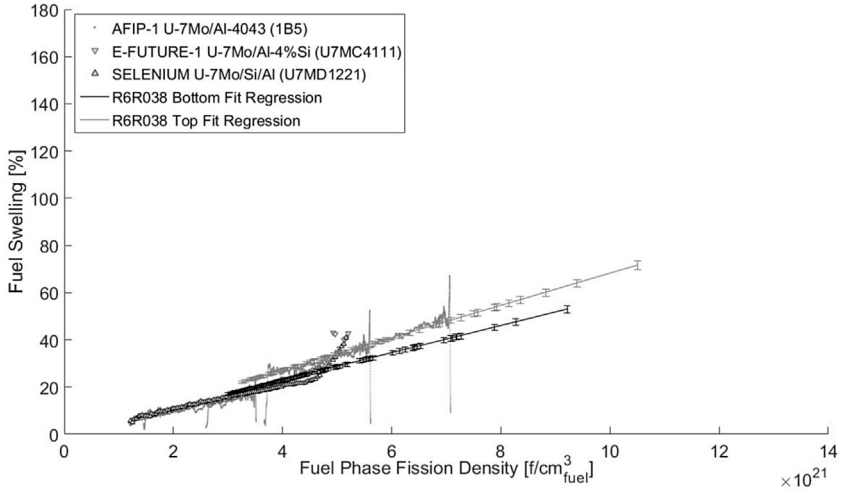

(c)

Fig. 12. (A) Plot of percent fuel swelling as a function of fuel phase fission density for fuel plate R6R038. (B) Linear Regression Plot of percent fuel swelling change as a function of fuel phase fission density for R6R038 including a 95% confidence band of the data. (C) Linear Regression Plot of percent fuel swelling change as a function of fuel phase fission density for R6R038 including a 95% confidence band of the fit. Data curves for fuel plates AFIP-1 1B5, E-FUTURE U7MC4111 and SELENIUM U7MD1221 are included for comparison on all plots.

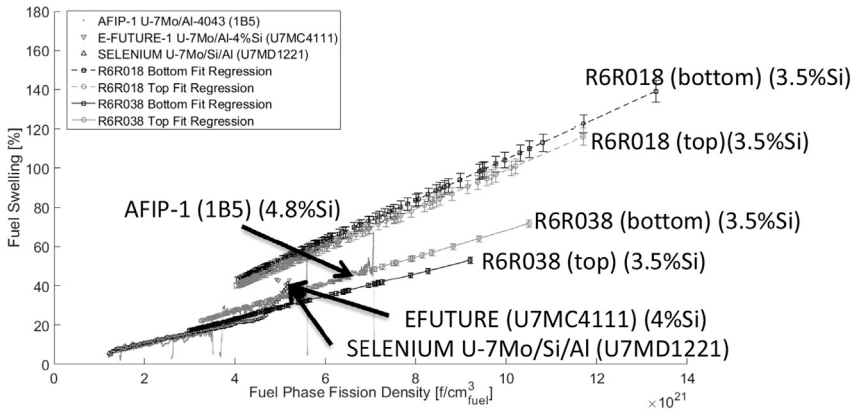

Fig. 13. Combined Linear Regression Plot of percent fuel swelling as a function of fuel phase fission density for R6R038 and R6R018. Data curves for fuel plates AFIP-1 1B5, E-FUTURE U7MC4111 and SELENIUM U7MD1221 are included for comparison on all plots.

Table 9
Calculated irradiation conditions for the R6R018 and R6R038 fuel plates compared to those reported for EFUTURE (U7MC 4111), SELENIUM (U7MD 1221), SELENIUM 1a, and AFIP-1 fuel plates [9].

Fuel Plate	Peak Heat Flux (W/cm^2)	Peak Fission Density (x10^{21} fissions/cm^3)	Peak Fission Rate (x10^{14} fissions/cm^3 sec)	EFPD
R6R018[a]	717	16.5	9.64	115
R6R038	582	12.7	8.38	115
SELENIUM 1221	466	5.3	8.89	69
EFUTURE 4111	457	5.5	8.27	77
SELENIUM 1a	350	5.6	6.61	98
AFIP-1	250	3.5	5.56	158

[a] The peak fuel irradiation parameters occur at the very edge of fuel plates R6R018 and R6R038, unlike the other fuel plates listed in the table.

The effect of the higher R6R018 fuel temperature at specific locations, in combination with the potential availability of more defects to support diffusion mechanisms, would be higher diffusion rates in the R6R018 fuel microstructure [12,13]. Under irradiation and in specific lower temperature regimes it does not take much change in temperature to result in noticeably higher rates of diffusion, and a resulting change in things like recrystallization, grain growth, fission gas mobility, creep, etc. Higher temperatures can also change the properties of the fuel and matrix materials (e.g., creep strength). As discussed by Duffin and Nichols [14], it is well established that when metals are irradiated they may, under certain conditions, show greatly increased deformation compared with unirradiated properties. This is the phenomenon known as irradiation creep and it is significant under conditions of relatively low temperature ($\leq$0.5 T_m), low stresses (less than post-irradiation yield stress) and high neutron flux ($\geq 10^{13}$ neutrons/cm^2 sec (>1 MeV)).

The different fuel swelling behavior for the R6R018 plate compared to EFUTURE fuel plate U7MC4111 and SELENIUM fuel plate U7MD1221 (not just in the rate of thickness change but also the discontinuous change in the rate at just over 4.5×10^{21} fissions/cm^3) could be impacted by the fact that these fuel plates were of a larger scale, were fabricated differently, had a different cladding with a different corrosion rate in-reactor, and were irradiated in the BR-2 reactor. The BR-2 reactor has a lower coolant pressure than does ATR [8], and other factors that may impact constraint effects were different. To understand the differences in swelling behavior for R6R018 compared to AFIP-1 fuel plate 1B5 it must be taken into account that the 1B5 measurements were performed using a an ultra-sonic scanner available in the ATR canal; it was larger-scale; it was manufactured by BWXT; it had a different starting microstructure (e.g., more fuel meat porosity, less interaction layer development around fuel particles); and it had differences in irradiation history (coolant flow, reactor core location, irradiation history, orientation relative to the core, etc.).

The R6R038 fuel plate showed better agreement with the swelling behavior of the EFUTURE, SELENIUM, SELENIUM 1a and AFIP-1 fuel plates, except the plot of its swelling behavior did not exhibit any deviation from linearity like the EFUTURE and SELENIUM fuel plates. The blistering observed for EFUTURE fuel plates, but not R6R018 and R6R038 fuel plates, could be the result of differences in irradiation history, fabrication processes, starting microstructure, cladding, corrosion, coolant pressure, constraint by the rails, or Si content in the fuel meat matrix. Also, the fact that EFUTURE was not an edge-on irradiation and was a larger fuel plate must be considered. Microstructural characterization using SEM and TEM is necessary to identify any differences between the aggressively-irradiated R6R018 fuel plate microstructure and the microstructure of other fuel plates. Destructive examination data is available for AFIP-1 [15], EFUTURE [16], SELENIUM [17], and SELENIUM 1a [9] fuel plates. Comparison of generated data may give indications as to how fuel performance phenomena at high fission rate/temperature may impact the rate of fuel plate thickness change for a fuel plate. For example, it could be dramatic changes in the swelling behavior of the fuel particles (i.e, formation of larger fission gas bubbles), significant growth of interaction layers, interconnection of porosity in the fuel meat, or a combination of some or all of these that result in relatively large fuel swelling.

5. Conclusions

Detailed thickness measurements were performed on two U-7Mo/Al-3.5Si dispersion fuel plates that were irradiated in the RERTR-9B experiment at different powers to similar fission densities, and based on these results the following conclusions can be made:

1.) A U-7Mo/Al-3.5Si dispersion fuel plate exhibits a higher rate of fuel swelling when it is irradiated at higher power, and the

increase in the observed swelling that occurs during irradiation is more pronounced at higher fission densities. Therefore as a fuel plate is irradiated, parameters other than just fission density seem to affect the swelling behavior of U-Mo/Al-Si dispersion fuels.

2.) Based on the fact that small and large-scale U-7Mo/Al-Si alloy matrix dispersion fuel plates never blistered during irradiation in the Advanced Test Reactor up to fission densities that exceed those achieved by fuel plates that blistered in the BR-2 reactor, parameters other than just fission density appear to impact the irradiation performance phenomena that lead to blistering of U-7Mo/Al-Si fuel plates.

U. S. Department of energy disclaimer

Acknowledgments

This work was supported by the U.S. Department of Energy, Office of Material Management and Minimization, National Nuclear Security Administration, under DOE-NE Idaho Operations Office Contract DE-AC07-05ID14517. This manuscript was authored by a contractor for the U.S. Government. The publisher, by accepting the article for publication, acknowledges that the U.S. Government retains a nonexclusive, paid-up, irrevocable, worldwide license to publish or reproduce the published form of this manuscript, or allow others to do so, for U.S. Government purposes. Personnel at the Hot Fuel Examination Facility at the Idaho National Laboratory are acknowledged for their assistance in performing the thickness measurements.

References

[1] M.K. Meyer, J. Gan, J.F. Jue, D.D. Keiser, E. Perez, A. Robinson, D.M. Wachs, N. Woolstenhulme, G.L. Hofman, Y.S. Kim, Irradiation performance of U-Mo monolithic fuel, Nucl. Engr. Tech 46 (2014) 169–182.

[2] Yeon Soo Kim, G.Y. Yeong, J.M. Park, A.B. Robinson, Fission induced swelling of U-Mo/Al dispersion fuel, J. Nucl. Mater 465 (2015) 142–152.

[3] D.R. Olander, Fundamental Aspects of Nuclear Reactor Fuel Elements, TID-26711–P1, Technical Information Center, Office of Public Affairs Energy Research and Development Administration, 1976.

[4] C.R. Clark, B.R. Muntifering, J.F. Jue, Production and characterization of atomized U-Mo powder by the rotating electrode, in: RERTR-2007 International Meeting on Reduced Enrichment for Research and Test Reactors, September 23-27, 2016. Prague Czech Republic.

[5] D.M. Perez, M.A. Lillo, G.S. Chang, G.A. Roth, N.E. Woolstenhulme, D.M. Wachs, RERTR-9 Irradiation Summary Report, Idaho National Laboratory, May 2011. INL/EXT-10–18421.

[6] S. Van den Berghe, Y. Parthoens, F. Charollais, Y.S. Kim, A. Leenaers, E. Koonen, V. Kuzminov, P. Lemoine, C. Jarousse, H. Guyon, D. Wachs, D. Keiser Jr., A. Robinson, J. Stevens, G. Hofman, Swelling of U(Mo)–Al(Si) dispersion fuel under irradiation – non-destructive analyses of the LEONIDAS E-FUTURE plates, J. Nucl. Mater 430 (2012) 246–258.

[7] S. Van den Berghe, Y. Parthoens, G. Cornelis, A. Leenaers, E. Koonen, V. Kuzminov, C. Detavernier, Swelling of U(Mo) dispersion fuel under irradiation – non-destructive analyses of the SELENIUM plates, J. Nucl. Mater 442 (2013) 60–68.

[8] D.M. Wachs, A.B. Robinson, F.J. Rice, N.C. Kraft, S.C. Taylor, M. Lillo, N. Woolstenhulme, G.A. Roth, Swelling of U-7Mo/Al-Si dispersion fuel plates under irradiation-Non-destructive analysis of the AFIP-1 fuel plates, J. Nucl. Mater 476 (2016) 270–292.

[9] A. Leenaers, Y. Parthoens, G. Cornelis, V. Kuzminov, E. Koonen, S. Van den Berghe, B. Ye, G.L. Hofman, Jason Schulthess, Effect of fission rate on the microstructure of coated UMo dispersion fuel, J. Nucl. Mater 494 (2017) 10–19.

[10] S.L. Hayes, M.K. Meyer, G.L. Hofman, J.L. Snelgrove, R.A. Brazner, Modeling RERTR experimental fuel plates using the plate code, in: 2003 International Meeting on Reduced Enrichment for Research and Test Reactors, October 5-10, 2003. Chicago, IL.

[11] A. Massih, Irradiation Induced Swelling of Nuclear Fuel, 1988. Swedish Nuclear Power Inspectorate Report, UK-88–127.

[12] G.J. Dienes, A.C. Damask, Radiation enhanced diffusion in solids, J. Appl. Phys. 29 (1958) 1713–1721.

[13] Y. Adda, M. Beyeler, G. Brebec, Radiation effects on solid state diffusion, Thin Solid Films 25 (1975) 107–156.

[14] W.J. Duffin, F.A. Nichols, The effect of irradiation on diffusion-controlled creep processes, J. Nucl. Mater 45 (1972/73), 302–216.

[15] D.D. Keiser Jr., J.F. Jue, A.B. Robinson, Microstructural development during irradiation of AFIP-1 fuel plates, in: RERTR 2010–32nd International Meeting on Reduced Enrichment for Research and Test Reactors, October 10-14, 2010. Lisbon, Portugal.

[16] A. Leenaers, S. Van den Berghe, J. Van Eyken, E. Koonen, F. Charollais, P. Lemoine, Y. Calzavara, H. Guyon, C. Jarousse, D. Geslin, D. Wachs, D. Keiser, A. Robinson, G. Hofman, Y.S. Kim, Microstructural evolution of U(Mo)–Al(Si) dispersion fuel under irradiation – destructive analyses of the LEONIDAS E-FUTURE plates, J. Nucl. Mater 441 (2013) 439–448.

[17] A. Leenaers, S. Van den Berghe, J. Van Eyken, E. Koonen, F. Charollais, P. Lemoine, Y. Calzavara, H. Guyon, C. Jarousse, D. Geslin, D. Wachs, D. Keiser, A. Robinson, G. Hofman, Y.S. Kim, Fuel swelling and interaction layer formation in the SELENIUM Si and ZrN coated U(Mo) dispersion fuel plates irradiated at high power in BR2, J. Nucl. Mater 458 (2015) 380–393.